



Effect of ionic liquids on kinetic parameters of dicyanate ester polycyclotrimerization and on thermal and viscoelastic properties of resulting cyanate ester resins

A. Fainleib, O. Grigoryeva, A. Vashchuk, O. Starostenko, S. Rogalsky, A. Rios de Anda, T-T-T. Nguyen, Daniel Grande

► To cite this version:

A. Fainleib, O. Grigoryeva, A. Vashchuk, O. Starostenko, S. Rogalsky, et al.. Effect of ionic liquids on kinetic parameters of dicyanate ester polycyclotrimerization and on thermal and viscoelastic properties of resulting cyanate ester resins. *Express Polymer Letters*, 2019, 13 (5), pp.469-483. 10.3144/expresspolymlett.2019.39 . hal-02062673

HAL Id: hal-02062673

<https://hal.science/hal-02062673>

Submitted on 5 Jul 2021

HAL is a multi-disciplinary open access archive for the deposit and dissemination of scientific research documents, whether they are published or not. The documents may come from teaching and research institutions in France or abroad, or from public or private research centers.

L'archive ouverte pluridisciplinaire **HAL**, est destinée au dépôt et à la diffusion de documents scientifiques de niveau recherche, publiés ou non, émanant des établissements d'enseignement et de recherche français ou étrangers, des laboratoires publics ou privés.

Effect of ionic liquids on kinetic peculiarities of dicyanate ester polycyclotrimerization and on thermal and viscoelastic properties of resulting cyanate ester resins

A. Fainleib^a, O. Grigoryeva^a, A. Vashchuk^{a,c}, O. Starostenko^a, S. Rogalsky^b, A. Rios de Anda,^c T.-T.-T. Nguyen^c, D. Grande^{c*}

^a*Institute of Macromolecular Chemistry, National Academy of Sciences of Ukraine, Kharkivske shose 48, 02160 Kyiv, Ukraine*

^b*Institute of Bioorganic Chemistry and Petrochemistry, National Academy of Sciences of Ukraine, Kharkivske shose 50, 02160 Kyiv, Ukraine*

^c*Institut de Chimie et des Matériaux Paris-Est, UMR 7182 CNRS – Université Paris-Est Créteil Val-de-Marne, 2, rue Henri Dunant, 94320 Thiais, France*

Abstract

A strong catalytic effect of 1.0 wt.% ionic liquids (ILs) on kinetic peculiarities of dicyanate ester of bisphenol E (DCBE) polycyclotrimerization was evidenced, and structure-property relationships of resulting densely cross-linked cyanate ester resins (CERs) were investigated. Three different ILs with contrasted reactivity were employed as a catalysts: an aprotic IL, *i.e.* 1-octyl-3-methyl imidazolium tetrafluoroborate ([OMIm][BF₄]), a protic IL, *i.e.* 2-(hydroxyethylamino) imidazolinium chloride ([HEAIm][Cl]), and a protic polymeric IL, *i.e.* poly(hexamethylene guanidine) toluene sulfonate ([PHMG][TS]). Both [HEAIm][Cl] and [PHMG][TS] were reactive towards DCBE monomer, whereas [OMIm][BF₄] was chemically inert, as confirmed by FTIR spectroscopy. Noticeably, the conversion (α_c) of cyanate groups in the presence of ILs dramatically increased, and a significant dependence of α_c values on IL chemical structure was found. The corresponding mechanisms of DCBE polycyclotrimerization in the presence of different ILs were proposed. All the CER/IL networks exhibited a high thermal stability inherent to neat CER, as shown by TGA, whereas unexpected significant changes of the viscoelastic characteristics for CER/IL networks compared to pure CER analogue was observed using DMTA.

Keywords: cyanate ester resins, ionic liquids, kinetics, catalytic effect, thermal stability, viscoelastic properties

*Corresponding author: Dr. Daniel Grande

Phone: +33 (0)1 49 78 11 77

E-mail: grande@icmpe.cnrs.fr

1. Introduction

Cyanate ester resins (CERs) represent a family of thermosetting polymers possessing attractive intrinsic features, such as excellent dimensional stability, high glass transition temperature ($T_g > 250^\circ\text{C}$), low dielectric constants (2.5-3.2), flame-retardancy, and high adhesion to conductor metals and composites. Therefore, they are promising materials for aerospace and microelectronic applications, especially as polymer matrices for structural composites, adhesives, potting resins, and coatings that work under severe conditions (high temperature, humidity, corrosive media, etc) [1-6]. Dicyanate ester monomers undergo thermal polycyclotrimerization to generate high T_g polycyanurate networks (PCNs), *i.e.* cyanate ester resins (CERs), without releasing volatile products. **Figure 1** describes the reaction scheme of polycyclotrimerization of one of the widely used monomers, *i.e.* dicyanate ester of bisphenol E (DCBE).

Dicyanate ester homopolymerization occurs at high temperature in the presence or the absence of a specific catalyst. The rate of non-catalyzed polycyclotrimerization is generally slow, and it depends on the concentration of impurities (traces of phenols and other residues from synthesis) [1]. Using a catalyst is necessary to achieve a controlled polycyclotrimerization process, which is a key factor for producing materials with excellent properties. This reaction is generally catalyzed by a combination of salts of transition metals, like acetyl acetonates of Cu, Co, Zn, Fe, Mn, Cr, etc. and an active hydrogen containing initiator like nonylphenol. Because of the well-known toxicity of phenolic compounds, attempts to find new effective catalysts for dicyanate ester polycyclotrimerization are of scientific and practical interest. In this regard, Throckmorton and Palmese [7] have found an acceleration of cyanate ester trimerization by dicyanamide-containing ionic liquids (ILs).

ILs are salts with melting points at temperatures below 100°C . They have attracted much attention due to their interesting properties, including negligible vapour pressure, large choice of salts liquid at room temperature, tunable physico-chemical characteristics, excellent thermal and chemical stability, selective solubility, ease of synthesis and good stability to oxidative and reductive conditions [8]. Since they are non-flammable, non-volatile and recyclable, they are greener alternatives to conventional organic solvents. Furthermore, they may be used as effective and reusable catalysts in some polymerization reactions [9-13] and

as initiators of free-radical [14,15] or cationic [16,17] polymerization processes. Thus, ILs have attracted widespread interest in polymer chemistry, due to their versatile properties [18,19]. In addition, ILs can also be suitable as porogens for producing nanoporous films and membranes, due to their high thermal stability and chemical inertness. In this regard, our teams have indeed successfully used 1-heptyl pyridinium tetrafluoroborate [HPyr][BF₄] as inert porogenic agent to produce nanoporous thermostable CER films [20].

Recently, our consortium has also found that an addition as small as 1.0 wt.% of the latter aprotic IL significantly accelerated the kinetics of DCBE polycyclotrimerization, which was explained by the formation of a [CN]^{δ+}[HPyr]^{δ-} complex as a key intermediate [21].

In the present paper, we thoroughly investigate the catalytic behaviour of three ILs with contrasted reactivity, namely an aprotic IL, *i.e.* [OMIm][BF₄], a protic IL, *i.e.* 2-(hydroxyethylamino) imidazolinium chloride ([HEAIm][Cl]), and a protic polymeric IL, *i.e.* poly(hexamethylene guanidine) toluene sulfonate ([PHMG][TS]), in thermosetting polymers. A comprehensive investigation of their effect on kinetic peculiarities (induction time, reaction time, monomer conversion degree, etc) of DCBE polycyclotrimerization as well as on thermal stability and viscoelastic properties of the resulting CERs is addressed.

2. Experimental

2.1. Materials

1,1-bis(4-cyanatophenyl) ethane (dicyanate ester of bisphenol E, DCBE), under the trade name PRIMASET™ LECy was kindly supplied by Lonza (Switzerland), and was used as received. The following chemicals (Fluka) were used as received for the synthesis of ILs: 1-methylimidazole, 1-bromooctane, 2-ethanolamine, tetrafluoroboric acid (50% in H₂O), ethyl acetate, hexane, methylene chloride, sodium sulfate, isopropanol, potassium hydroxide, guanidine hydrochloride, hexamethylenediamine, 0.1 N sodium chloride, sodium toluenesulfonate, and ethanol.

2.2. Synthesis of ionic liquids

2.2.1. Synthesis of 1-octyl-3-methyl imidazolium tetrafluoroborate ([OMIm][BF₄])

[OMIm][BF₄] ionic liquid was synthesized using literature methods previously described [22,23]. The stirred mixture of 1-bromooctane (27 g, 0.14 mol) and 1-methylimidazole (10 g,

0.12 mol) was heated at 140°C for 2 h under argon atmosphere. The viscous liquid of light brown color obtained was cooled to room temperature and washed with ethyl acetate-hexane mixture (3:1 (v/v), 3×100 mL). Residual solvents were removed at reduced pressure and the obtained product was dissolved in 150 mL of water. Tetrafluoroboric acid (25 mL) was added to the solution followed by stirring for 1 h. The immiscible aqueous layer formed was extracted with methylene chloride (2×100 mL), and dried overnight with sodium sulfate. The solvent was distilled off, and the resulting ionic liquid was dried under reduced pressure of 1 mbar at 80°C for 12 h. The product yield was equal to 72 %.

¹H NMR (300 MHz, CDCl₃): δ (ppm): 0.86 (t, 3H, CH₃, J=7.2 Hz), 1.25-1.31 (m, 9H, CH₂), 1.86 (m, 3H, CH₂), 3.94 (s, 3H, NCH₃), 4.16 (t, 2H, NCH₂, J=7.2 Hz), 7.27-7.38 (m, 2H, NC(H)C(H)N), 8.78 (s, 1H, NC(H)N).

¹⁹F NMR (188 MHz, CDCl₃): δ (ppm): -151.4.

¹H NMR (300 MHz, DMSO-*d*₆, TMS): δ (ppm): 0.85 (t, 3H, CH₃), 1.25 (m, 10H, CH₃(CH₂)₅), 1.78 (m, 2H, NCH₂CH₂), 3.85 (s, 3H, NCH₃), 4.16 (t, 2H, NCH₂), 7.67 (br s, 1H, C₄-H), 7.74 (br s, 1H, C₅-H), 9.06 (s, 1H, C₂-H).

¹⁹F NMR (188 MHz, DMSO-*d*₆, CFCl₃): δ (ppm): -148.8 (s, 4F, BF₄).

2.2.2. Synthesis of 2-(hydroxyethylamino) imidazolinium chloride ([HEAIm][Cl])

2-methylmercaptoimidazoline-2-chlorohydrate was obtained according to a literature method [24].

¹H NMR (300 MHz, DMSO-*d*₆): δ (ppm): 2.71 (s, 3H, CH₃), 3.84 (s, 4H, CH₂), 10.64 (2H, br s, NH).

The stirred mixture of 2-methylmercaptoimidazoline-2-chlorohydrate (5 g, 0.032 mol) and 2-ethanolamine (2.1 g, 0.035 mol) in 50 mL of isopropanol was heated to boiling for 6 h. Methylmercaptane formed as by-product was absorbed by 20 % water solution of potassium hydroxide. The solvent was removed at reduced pressure and the obtained solid residue of [HEAIm][Cl] was purified by double recrystallization from isopropanol. Yield: 85 %.

¹H NMR (300 MHz, DMSO-*d*₆): δ (ppm): 3.25 (m, 2H, CH₂OH), 3.56 (m, 6H, NHCH₂CH₂OH), 7.64 (4H, br s, NH, OH)

2.2.3. Synthesis of poly(hexamethylene guanidine) toluene sulfonate ([PHMG][TS])

The mixture of guanidine hydrochloride (10 g, 0.104 mol) and hexamethylene diamine (11.7 g, 0.1 mol) was heated at 100°C for 4 h under constant stirring. Further, the reaction was carried out for 4 h at 140°C, 4 h at 180°C and 3 h at 200°C to obtain a highly viscous liquid.

After cooling the reaction mixture to room temperature, the vitreous solid of poly(hexamethylene guanidine) hydrochloride obtained ([PHMG][Cl]) was dissolved in water (150 mL), filtered and precipitated by addition of saturated water solution of sodium chloride (50 mL). The polymer was isolated by decantation of water solution, dried at 140°C for 24 h and ground in a porcelain mortar. The intrinsic viscosity was equal to 7 cm³/g for [PHMG][Cl] solution in 0.1 M sodium chloride at 25°C.

¹H NMR (300 MHz, DMSO-*d*₆): δ (ppm): 1.3-1.44 (m, 8H, (CH₂)₄), 3.14 (m, 4H, (N-CH₂)₂), 7.15-7.8 (br s, 4H, C-NH, C=NH₂⁺).

Elemental analysis: (C₇H₁₆N₃Cl)_x (177.5)_x: calculated (%): C 47.3, H 9.0, N 23.6, Cl 20.0; found (%): C 46.7, H 8.6, N 24.1, Cl 20.6.

Sodium toluene sulfonate (11.4 g, or 0.058 mol) was added to a solution of [PHMG][Cl] (10 g, 0.056 mol) in 100 mL of ethanol, and the mixture was stirred for 20 h at room temperature. The resulting sodium chloride precipitate was filtered off, and the filtrate was poured into water (300 mL). The white slurry was separated by decantation, followed by washing with water. It was dried at 120-130°C for 24 h and ground to obtain [PHMG][TS] as a powder.

¹H NMR (300 MHz, DMSO-*d*₆): δ (ppm): 1.24 (m, 4H, (CH₂)₂), 1.42 (m, 4H, NCH₂CH₂), 2.29 (s, 3H, TsO-CH₃), 3.14 (m, 4H, (NCH₂)), 7.14 (d, 2H, H-3, H-5), 7.3-7.35 (br s, 4H, C-NH, C=NH₂⁺), 7.53 (d, 2H, H-2, H-6).

Elemental analysis: (C₁₄H₂₃N₃O₃S)_x (313)_x: calculated: C 53.6, H 7.3, N 13.4, S 10.2; found: C 53.1, H 7.0, N 13.8, S 10.5.

The chemical structure and some physico-chemical characteristics of individual components used in this study are summarized in **Table 1**. The solubility parameters (δ) of DCBE and ILs were calculated according to Fedor's Group Contribution Method [25].

2.3. Preparation of CER-based networks

Mixtures of DCBE with 1.0 wt.% IL were first stirred until homogeneous state as follows. DCBE monomer was mixed with [OMIm][BF₄], [HEAIm][Cl] or [PHMG][TS] at *T* ~ 150°C for ~3 min, then the homogeneous DCBE/IL mixtures were polymerized by a step-by-step curing procedure with the following successive heating conditions: 150°C/8 h, 180°C/3h, 210°C/3 h, 230°C/1 h.

The effect of IL chemical structure on the resulting CER/[OMIm][BF₄], CER/[HEAIm][Cl] or CER/[PHMG][TS] networks was studied by FTIR to detect possible chemical reactions between OCN groups of DCBE and functional groups of ILs. A model composition for DCBE/IL equal to 50/50 wt.% was used at 150°C for 3 min to obtain homogeneous mixtures, followed by a step-by-step curing procedure with the following heating conditions: 150°C/8 h, 180°C/3 h, 210°C/3 h, 230°C/1 h.

2.4. Physico-chemical techniques

¹H NMR and ¹⁹F NMR techniques were used to characterize the ionic liquids synthesized. The spectra were recorded with a Varian (300 MHz) NMR spectrometer at 23°C using DMSO-*d*₆ as the deuterated solvent.

Elemental analysis of the ionic liquids synthesized was performed using classical approaches described elsewhere [24].

For kinetic measurements by FTIR, neat DCBE or DCBE/IL mixtures of 99/1 wt.% compositions were poured directly onto NaCl windows, followed by their isothermal heating in a temperature-controlled oven at 150°C for 8 h with periodic sampling out (every 30 min). FTIR spectra were recorded at room temperature between 4000 and 600 cm⁻¹ using a Bruker Tensor 37 spectrometer. For each spectrum, 32 consecutive scans with a resolution of 4 cm⁻¹ were averaged.

The IR band at 1500 cm⁻¹ of benzene ring vibrations was used as an internal standard. DCBE conversion was determined by monitoring the disappearance of –O–C≡N stretching band at 2266 cm⁻¹. The conversion (α_c) of cyanate groups was calculated using Equation 1:

$$\alpha_c = \left(1 - \frac{I_{(t)2266} / I_{(0)2266}}{I_{(t)1500} / I_{(0)1500}}\right) \times 100 \quad (1)$$

where $I_{(t)2266}$ is the intensity of C≡N vibration band in –O–C≡N at 2266 cm⁻¹ at time t ; $I_{(t)1500}$ is the intensity of carbon-carbon stretching vibrations in aromatic ring band at 1500 cm⁻¹ at time t ; $I_{(0)}$ is the intensity of corresponding vibration bands in the initial DCBE-containing mixture.

Thermogravimetric analysis (TGA) measurements were performed using a Setaram SETSYS evolution 1750 thermobalance. Samples were heated in a platinum crucible from 20 to 700°C at a heating rate of 10°C·min⁻¹ under argon atmosphere. The sample mass was about 10 mg.

Dynamic mechanical thermal analysis (DMTA) was carried out using a DMA-Q800 equipment (TA Instruments) in a temperature range from 20 to 350°C at a heating rate of 4°C/min and frequency values of 1, 3, 5, 10, 15 and 20 Hz using single cantilever bending mode. Rectangular samples of size 40×5×1 mm were tested.

The apparent activation energy (ΔE_a) for α relaxation was determined by applying the Vogel-Fulcher-Tammann (VFT) equation as follows (Equation 2) [26-29]:

$$f = f_0 \exp \left[-\frac{\Delta E_a}{R(T - T_{VFT})} \right] \quad (2)$$

where f represents the frequency, f_0 is analogous to the rate constant and pre-exponential factor of Arrhenius Equation, R is the gas constant ($R = 8.314 \cdot 10^{-3} \text{ kJ} \cdot \text{mol}^{-1} \cdot \text{K}^{-1}$), T stands for absolute temperature, T_{VFT} is about 50°C lower than the α transition temperature T_α .

The shift of α relaxation temperatures ($T_{\alpha 1}$ and $T_{\alpha 2}$) due to changes in the test frequencies (f_1 and f_2) allows for the determination of ΔE_a values by using Equations 3, 4 and 5 [30]:

$$\frac{f_1}{f_2} = \frac{\exp\left(\frac{-\Delta E_a}{R(T_{\alpha 1} - T_{VFT})}\right)}{\exp\left(\frac{-\Delta E_a}{R(T_{\alpha 2} - T_{VFT})}\right)} \quad (3)$$

$$\log \frac{f_1}{f_2} = \log a_T = \frac{\Delta E_a}{R} \left[\frac{1}{(T_{\alpha 2} - T_{VFT})} - \frac{1}{(T_{\alpha 1} - T_{VFT})} \right] \quad (4)$$

$$\Delta E_a = -R \frac{d \ln f}{d\left(\frac{1}{T_\alpha - T_{VFT}}\right)} \quad (5)$$

3. Results and discussion

3.1. Kinetic investigation by FTIR

Kinetics of neat CER formation and DCBE polymerization in the presence of [OMIm][BF₄], [HEAIm][Cl] or [PHMG][TS] was investigated by FTIR. The normalized FTIR spectra of corresponding networks during their isothermal curing at 150°C are shown in **Figure 2**. The

absorption doublet at 2266-2237 cm^{-1} corresponding to $-\text{O}-\text{C}\equiv\text{N}$ group stretching vibrations diminished with the curing time for pure CER as well as for all the CER/IL networks, while the bands at 1565 and 1369 cm^{-1} , respectively corresponding to valence vibrations of $\text{C}=\text{N}$ bonds ($\nu_{\text{C}=\text{N}}$) in $\text{C}=\text{N}-\text{C}$ groups and $\text{N}-\text{C}$ bonds ($\nu_{\text{N}-\text{C}}$) in $\text{N}-\text{C}-\text{O}$ groups of cyanurate cycles, appeared [1,2].

The time dependence of cyanate group conversion (α_c) and reaction rate ($W = d\alpha/dt$) for neat CER and CER/IL networks is shown in **Figure 3**. For pure CER, the induction period of DCBE polycyclotrimerization was equal to about 60 min, whereas for CER/[OMIm][BF₄], CER/[HEAIm][Cl] and CER/[PHMG][TS], the induction period was by 1.5-3.0 times shorter, depending on IL structure (**Table 2**). In addition, the maximal rate of reaction, W_{max} , increased by 10-20 % and the time to maximal rate of reaction, t_{max} , decreased by 7-42 % (**Table 2**). Therefore, the introduction of ILs into the DCBE reaction medium significantly accelerated the conversion of $-\text{O}-\text{C}\equiv\text{N}$ groups from the early stages of CER network formation. It should be noticed that conversion of $-\text{O}-\text{C}\equiv\text{N}$ groups reached the value of $\alpha_c \sim 0.98$ for all the CER networks synthesized after the complete curing schedule.

Further, for all CER-based systems, the reaction rate increased dramatically in the kinetic-controlled stage (linear part of conversion vs. time curve in **Figure 3a**) until it reached a maximum W_{max} (**Figure 3b**). After reaching the gel point, the reaction rate decreased drastically as the polymerization process became diffusion-limited. For all the CER/IL networks, the reaction was faster compared to neat CER (completion after about 360 min).

3.2. CER/IL curing mechanisms

The curing mechanisms of CER/IL composites were studied on model reactions starting from DCBE/IL mixtures with a 50/50 wt.% composition. The spectrum of CER/[OMIm][BF₄] showed only characteristic absorbance bands of both individual components (see **Figure 4**, curve **3**) that evidenced the chemical inertness of [OMIm][BF₄] towards DCBE. In a previous work [31], we have already proposed the mechanism of DCBE polymerization in the presence of [OMIm][BF₄] *via* the formation of a $[\text{CN}]^{\delta+}-[\text{OMIm}]^{\delta-}$ complex as a key intermediate (**Figure 5**).

One could suppose the same mechanism for DCBE polymerization in the presence of [HEAIm][Cl]. However, in the latter case, the competition between the catalytic complex formation and the covalent bonding through the reaction of cyanate groups of DCBE with –OH and >NH groups of [HEAIm][Cl] should be considered. Thus, a three-step mechanism was proposed for the formation of cyanurate cycles from DCBE polymerization being catalyzed by [HEAIm][Cl] (**Figure 6**). Our hypothesis was based on the well-known mechanisms of polycyclotrimerization of CERs in the presence of hydroxy [1,32-35] and amino [36,37] compounds. First, during the mixing procedure, the –OCN groups of DCBE could react with hydroxyl groups of [HEAIm][Cl] with formation of imidocarbonate O–C(=NH)–O fragment (**Figure 6**, compound **2**), which further reacted with a second DCBE molecule with formation of a stabilized dimer (**Figure 6**, compound **3**). A third DCBE molecule reacted with the dimer **3**, thus giving rise to the intermediate **4**, which was further transformed into the triazine ring. This transformation could be potentially followed by two mechanisms: either [HEAIm][Cl] release leading to product **5** (cyanurate cycle) or [HEAIm][Cl] incorporation directly into the cyanurate network (**Figure 6**, compound **6**) with release of ROH (monocyanate of bisphenol A). According to Grigat and Putter [36] as well as our previous works [33-35], the more acidic phenol compared to alcohol was released, and thus, a substituted triazine ring should be obtained with the release of a monophenol derived from DCBE. Moreover, we presumed that [HEAIm][Cl] could also increase the polarization of the C=N bond in the imidocarbonate (**Figure 6**, compound **2**), thus making the carbon atom of this functional group more electrophilic. This was confirmed by FTIR through the appearance of a shoulder at 1440 cm⁻¹ attributed to N–C=O asymmetric vibrations along with a band at 1706 cm⁻¹, which could be related to C=O stretching vibrations in the urea linkage of imidazolidinone (**Figure 6**, compound **4'**; see **Figure 4**, curve **6**) [38]. The formation of compound **4'** from **2** might be possible upon releasing of monophenol derivative through the formation of iminooxazolidine **3'**, which could also be accompanied by its partial isomerization into compound **4'**. Furthermore, the reaction between the secondary >NH groups of [HEAIm][Cl], which were less reactive than –OH groups, was possible as well. The occurrence of structure **3'** was confirmed by FTIR with the appearance of a shoulder at 1633 cm⁻¹ assigned to the N–H in the isourea linkage [39] (see **Figure 4**, curve **6**), which seemed to be formed together with the cyanurate-based compounds (**Figure 6**, compounds **5** and **6**). Accordingly, hybrid chemical structures with additional network junctions could be produced for the CER/[HEAIm][Cl] system.

The proposed mechanism of DCBE polycyclotrimerization process in the presence of [PHMG][TS] was also based on the reactivity of secondary amino groups towards cyanate groups, as represented schematically in **Figure 7**. The new strong absorption FTIR bands around 1565 and 1369 cm^{-1} could be attributed to the C=N–C and O–C–N stretching vibrations in cyanurate groups. Two routes of grafting of [PHMG][TS] polymer chains onto the CER network structure were possible. Meanwhile, the existence of a new group conjugated to a triazine ring was proved by the FTIR bands at around 1544 cm^{-1} ($\nu_{\text{C=N}}$) [40] and 1512 cm^{-1} attributed to aromatic ring stretching vibrations (**Figure 7**, compound **3'**; see **Figure 4**, curve 9). The absorption band at 1391 cm^{-1} could be assigned to the stretching vibrations $\nu_{\text{N-C}}$ [41] associated with groups bridging the triazine rings (**Figure 7**, compound **4**). All these observations confirmed the [PHMG][TS] incorporation into the polycyanurate network structure.

Additionally, a band at 1772 cm^{-1} attributed to C=O stretching vibrations appeared in the FTIR spectra of both initial DCBE/[PHMG][TS] mixture and CER/[PHMG][TS] after complete curing (see **Figure 4**, curves **8** and **9**). We could suppose that the reaction of cyanate groups from DCBE and CER with traces of water [42] or phenolic impurity could occur to generate an imidocarbonate intermediate (**Figure 8**).

3.3. Thermal stability of CER-based networks by TGA

The thermal stability of CER/IL networks as well as individual components (*i.e.*, neat CER and ILs) was investigated by TGA (**Figure 9**, **Table 3**). It is noteworthy that all CER/ILs networks exhibited high thermal stability, similarly to pure CER, as no visible mass loss was observed at temperatures below 420°C. For all the CER-based networks, the main degradation stage occurred in a temperature range from $T_{\text{d onset}} \approx 420\text{--}427^\circ\text{C}$ to $T_{\text{d end}} \approx 450\text{--}460^\circ\text{C}$, depending on IL structure. One could also observe some weak degradation stage in a temperature range of $T \approx 500\text{--}640^\circ\text{C}$ for all the samples under investigation, which could be attributed to CER mass loss due to the elimination of alkenes and hydrogen, leaving a carbonaceous char containing residual oxygen and nitrogen [43,44].

The thermal stability of CER/[OMIm][BF₄] and CER/[HEAIm][Cl] was quite similar to that of neat CER (see **Figure 9**, **Table 3**). This meant that using 1.0 wt.% of corresponding ILs did not change significantly the chemical structure and cross-linking density of the CER network. We considered that one such behaviour resulted from the fact that [OMIm][BF₄] had no

chemical bonds with the CER network (cf. **Figure 5**). [HEAIm][Cl] had a covalent grafting with the cyanurate network but the molecular mass of the IL molecules was too small ($M = 164$ g/mol, see **Table 1**), and above all, an amount of 1.0 wt.% was too low to significantly change the chemical structure and notably the cross-linking structure of the CER matrix. Interestingly, despite a thermal stability of pure [HEAIm][Cl] substantially lower than that of other ILs and neat CER (**Figure 9b**, **Table 3**), the careful analysis of the TGA curve of the CER/[HEAIm][Cl] network did not show the corresponding mass loss (*i.e.* 1.0 wt.%) of the IL in the temperature range in which the main degradation of pure IL occurred. Therefore, the highly crosslinked CER network might prevent the IL from regular thermal degradation, probably due to its chemical incorporation into the CER matrix (see **Figure 6**).

On the contrary, the CER/[PHMG][TS] network was characterized by a lower thermal stability compared to the other analogues (cf. **Table 3**). Obviously enough, one such behaviour might arise from the formation of a CER network with lower cross-linking density and structural regularity, due to the chemical incorporation of relatively long linear polymer fragments of [PHMG][TS] ($M_n = 12,520$ g/mol, see **Table 1**) into the CER matrix.

3.4. Viscoelastic properties of CER-based networks by DMTA

Figure 10 shows the temperature dependence of storage modulus (E') and loss factor ($\tan\delta$) for neat CER and CER/IL networks. All the samples were characterized by high α relaxation temperature values ($T_\alpha > 240^\circ\text{C}$, **Table 4**), as typically found for thermostable cross-linked polymers, due to high temperature resistance of cross-links and high cross-linking density of polymer networks [1-6,32-35].

Unpredictably, a significant effect of the low IL content (*i.e.*, 1.0 wt.%) on the viscoelastic properties of all CER/IL networks was found compared to those of pure CER (**Figure 10**, **Table 4**). As expected, the lowest changes were observed for the CER/[OMIm][BF₄] network. This was probably due to the fact that the IL was not chemically embedded into the CER network structure. Nevertheless, a slight decrease in T_α and E' values as well as an increase in $\tan\delta_{\max}$ and ΔT values were evidenced, thus demonstrating a higher mobility of the kinetic segments between the cross-links of the CER matrix.

On the contrary, the chemical incorporation of [HEAIm][Cl] and especially [PHMG][TS] into the CER matrix resulted in a substantial decrease in the values of T_α as well as a significant rise in values of $\tan\delta_{\max}$ and ΔT compared to those for neat CER. Again, these facts evidenced the increase in mobility of the kinetic segments within the CER matrix, due to the reduced cross-linking density of the polycyanurate network in the CER/IL samples. Such changes turned out to be more drastic for the CER/[PHMG][TS] network, due to the chemical incorporation of polymeric chains from the IL into the CER network compared to the grafting of small molecules of [HEAIm][Cl] into the corresponding CER matrix. For the CER/[PHMG][TS] network, a dramatic decrease in E' values was observed in the whole glassy region up to 235°C (**Figure 10a**, **Table 4**), which confirmed the aforementioned conclusion on the formation of a CER matrix with more structural defects compared to all other analogues.

Furthermore, the changes in values of apparent activation energy of α relaxation (ΔE_a) calculated for all the samples (**Table 4**) confirmed the aforementioned observations. First of all, the temperature dependence of frequency, *i.e.* plots of $\log f$ vs. $(1000/T)$ (**Figure 11**), displayed a steep linearity in the region close to 1 Hz ($f = 1.0$ -20.0 Hz), which is typical of the α relaxation. For higher f values (at around 10^3 Hz and above), this linearity was lost. From these plots, reliable values of ΔE_a were determined. Indeed, the E_a value can be translated as the amount of energy required to activate the molecular motion and rearrangement of some molecular segments around T_α [45,46]. The E_a value for the CER/[OMIm][BF₄] network was very close to that for pure CER ($\Delta E_a \approx 286$ kJ/mol and $\Delta E_a \approx 292$ kJ/mol, respectively), thus corroborating a similar main transition process related to similar cross-linked structures in both samples because the IL was not chemically embedded into the network. The observed decline in ΔE_a values for CER/[HEAIm][Cl] ($\Delta E_a \approx 255$ kJ/mol) and CER/[PHMG][TS] ($\Delta E_a \approx 196$ kJ/mol) was consistent with the hypothesis of the formation of hybrid CER/IL networks with lower cross-linking density and more mobile kinetic segments between junctions due to the chemical incorporation of the ILs into the CER matrix.

For the CER/[PHMG][TS] network, it is noteworthy that in the $\tan\delta = f(T)$ curve, a second $\tan\delta$ peak was also observed at 284°C, which could be explained by the post-curing process occurring in the CER matrix, while heating the sample during DMTA measurements above T_α ($T > 240^\circ\text{C}$) [47], due to reaction of high mobility residual $-\text{O}-\text{C}\equiv\text{N}$ groups in the hybrid

CER/[PHMG][TS] network. Interestingly, a noticeable increase in the E' modulus above T_α (**Figure 10a**) for all the networks was also caused by a post-curing effect which occurred upon heating the samples during DMTA measurements, resulting in some increase in the final cross-linking density of CER/IL networks. As it could be seen from **Table 4**, the post-curing started at different temperatures ($T_{pc(onset)}$) for the different samples: one could assume that the lower the cross-linking density of the cured network, the higher the mobility of the residual $-\text{O}-\text{C}\equiv\text{N}$ groups from CER, and the lower the onset temperature of post-curing.

4. Conclusions

This paper thoroughly discussed the kinetic peculiarities of DCBE polycyclotrimerization in the presence of very small amounts (*i.e.* 1.0 wt.%) of ionic liquids with contrasted reactivity, *i.e.* an aprotic IL ([OMIm][BF₄]), a protic IL ([HEAIm][Cl]), and a protic polymeric IL ([PHMG][TS]). Further, the relationships between the structure of the densely cross-linked CER/IL networks and their thermal and viscoelastic properties were compared to those associated with neat CER. A strong catalytic effect of all ILs used on DCBE polycyclotrimerization leading to CER network formation was found, and the IL catalytic activity could be ranked as follows: aprotic [OMIm][BF₄] > protic [HEAIm][Cl] > protic polymeric [PHMG][TS]. Plausible mechanisms for all the DCBE/IL systems were proposed to explain the acceleration effect of the ILs.

One such acceleration effect was significantly higher in the presence of [OMIm][BF₄], due to its chemical inertness towards DCBE monomer. In the case of [HEAIm][Cl] and [PHMG][TS], the chemical grafting of the ILs to CERs might occur. The polymer segment mobility and activation energy (E_a) for α relaxation were studied using DMTA for neat CER and CER/ILs networks. All the samples exhibited a high T_α (*i.e.*, 242-262°C at 1.0 Hz). It was found that the physical incorporation of [OMIm][BF₄] into the CER network had no significant influence on T_α value compared to that of neat CER. On the contrary, the chemical incorporation of both [HEAIm][Cl] and [PHMG][TS] resulted in the significant decrease of T_α values for corresponding CER/IL networks caused by the formation of hybrid chemical structures with lower structural regularity than that of neat CER. Nevertheless, TGA results

revealed that the catalytic amounts of ILs had no major influence on the thermal stability of CER-based networks compared to pure CER.

Accordingly, catalytic amounts of ILs used for the synthesis of CER thermosetting materials do not impair their main thermal characteristics, thus keeping their applicability as suitable matrices for aerospace composites or microelectronic devices.

Acknowledgments

The authors gratefully acknowledge the National Academy of Sciences of Ukraine (NASU) and the “Centre National de la Recherche Scientifique” (CNRS) of France for partial financial support (French-Ukrainian LIA project). They are also indebted to the Campus France for the Eiffel grant N°870769C provided to A. Vashchuk and for the grant N°882170D provided to Prof. A. Fainleib for respective stays at the ICMPE.

References

- [1] Hamerton I. Chemistry and technology of cyanate ester resins. Chapman & Hall, Glasgow (1994).
- [2] Fainleib A. Thermostable polycyanurates: synthesis, modification, structure and properties. Nova Science Publishers, New York (2010).
- [3] Goertzen W. K., Kessler M. R. Thermal and mechanical evaluation of cyanate ester composites with low-temperature processability. Composites Part A: Appl. Sci. Manufacturing, **38**, 779-784 (2007).
[DOI: 10.1016/j.compositesa.2006.09.005](https://doi.org/10.1016/j.compositesa.2006.09.005)
- [4] Fang T., Shimp D. A. Polycyanate esters: Science and applications. Prog. Polym. Sci., **20**, 61-118, (1995).
[DOI: 10.1016/0079-6700\(94\)E0006-M](https://doi.org/10.1016/0079-6700(94)E0006-M)
- [5] Fainleib A., Bardash L., Boiteux G., Grigoryeva O. Thermosetting Cyanate Ester Resins Filled with CNTs. In “*Advances in progressive thermoplastic and thermosetting polymers, perspectives and applications*” (Ye. Mamunya, and M. Iurzhenko, editors), Tehnopress editura, Iasi, Romania, 2012, Chapter 10, p. 379-424.

- [6] Grande D., Grigoryeva O., Fainleib A., Gusakova K., Lorthioir C. Porous thermosets via hydrolytic degradation of poly(ϵ -caprolactone) fragments in cyanurate-based hybrid networks. *Eur. Polym. J.*, **44**, 3588-3598 (2008).
[DOI: 10.1016/j.eurpolymj.2008.08.041](https://doi.org/10.1016/j.eurpolymj.2008.08.041)
- [7] Throckmorton J., Palmese G. Acceleration of cyanate ester trimerization by dicyanamide RTILs. *Polymer*, **91**, 7-13 (2016).
[DOI: 10.1016/j.polymer.2016.03.019](https://doi.org/10.1016/j.polymer.2016.03.019)
- [8] Handy S. T. Room temperature ionic liquids: Different classes and physical properties. *Curr. Org. Chem.*, **9**, 959-988 (2005).
[DOI: 10.2174/1385272054368411](https://doi.org/10.2174/1385272054368411)
- [9] Pârvulescu V. I., Hardacre C. Catalysis in ionic liquids. *Chem. Rev.*, **107**, 2615-2665 (2007).
[DOI 10.1021/cr050948h](https://doi.org/10.1021/cr050948h)
- [10] Wasserscheid P., Welton T. *Ionic liquids in synthesis*. VCH-Wiley, Weinheim (2002).
- [11] Zhou J., Cheng L, Wu D. Ring-opening polymerization of ethylene carbonate using ionic liquids as catalysts. *e-Polymers*, **11**, 883-891 (2011).
[DOI: 10.1515/epoly.2011.11.1.883](https://doi.org/10.1515/epoly.2011.11.1.883)
- [12] Kaoukabi A., Guillen F., Qayouh H., Bouyahya A., Balieu S., Belachemi L., Gouhier G., Lahcini M. The use of ionic liquids as an organocatalyst for controlled ring-opening polymerization of ϵ -caprolactone. *Industrial Crops Products*, **72**, 16-23 (2015).
[DOI: 10.1016/j.indcrop.2015.02.002](https://doi.org/10.1016/j.indcrop.2015.02.002)
- [13] Abdolmaleki A., Mohamadi Z. Acidic ionic liquids catalyst in homo and graft polymerization of ϵ -caprolactone. *Colloid Polym. Sci.*, **291**, 1999-2005 (2013).
[DOI: 10.1007/s00396-013-2941-x](https://doi.org/10.1007/s00396-013-2941-x)
- [14] Ding S., Radosz M., Shen Y. Ionic liquid catalyst for biphasic atom transfer radical polymerization of methyl methacrylate. *Macromolecules*, **38**, 5921-5928 (2005).
[DOI: 10.1021/ma050093a](https://doi.org/10.1021/ma050093a)
- [15] Kanno S. Challenges for unique application of ionic liquids as a novel initiator of radical polymerization. *Molecular Cryst. Liquid Cryst.*, **603**, 1-3 (2014).
[DOI: 10.1080/15421406.2014.966234](https://doi.org/10.1080/15421406.2014.966234)
- [16] Yang F., Yang J., Zheng K., Stansbury J. W., Nie J. Electro-induced cationic polymerization of vinyl ethers by using ionic liquid 1-butyl-3-methylimidazolium tetrafluoroborate as initiator. *Macromol. Chem. Phys.*, **216**, 380-385 (2015).
[DOI: 10.1002/macp.201400467](https://doi.org/10.1002/macp.201400467)

[17] Wu Y., Han L., Zhang X., Mao J., Gong L., Guo W., Gu K., Li S. Cationic polymerization of isobutyl vinyl ether in an imidazole-based ionic liquid: characteristics and mechanism. *Polym. Chem.*, **6**, 2560-2568 (2015).

[DOI: 10.1039/C4PY01784F](https://doi.org/10.1039/C4PY01784F)

[18] Livi S., Duchet-Rumeau J., Gérard J. F., Pham T. N. Polymers and ionic liquids: a successful wedding. *Macromol. Chem. Phys.*, **216**, 359-368 (2015).

[DOI: 10.1002/macp.201400425](https://doi.org/10.1002/macp.201400425)

[19] Vashchuk A., Fainleib A., Starostenko O., Grande D. Application of ionic liquids in thermosetting polymers: epoxy and cyanate ester resins. *eXPRESS Polym. Lett.*, **12**, 898-917 (2018)

[DOI: 10.3144/expresspolymlett.2018.77](https://doi.org/10.3144/expresspolymlett.2018.77)

[20] Fainleib A., Vashchuk A., Starostenko O., Grigoryeva O., Rogalsky S., Nguyen T. T., Grande D. Nanoporous polymer films of cyanate ester resins designed by using ionic liquids as porogens. *Nanoscale Res. Lett.*, **12**, p.1-9 (2017).

[DOI: 10.1186/s11671-017-1900-8](https://doi.org/10.1186/s11671-017-1900-8)

[21] Vashchuk A., Rios de Anda A., Starostenko O., Grigoryeva O., Sotta P., Rogalsky S., Smertenko P., Fainleib A., Grande D. Structure-Property relationships in nanocomposites based on cyanate ester resins and 1-heptyl pyridinium tetrafluoroborate ionic liquid. *Polymer*, **148**, 14-26 (2018)

[DOI: 10.1016/j.polymer.2018.06.015](https://doi.org/10.1016/j.polymer.2018.06.015)

[22] Dzyuba S. V., Bartsch R. A. Efficient synthesis of 1-alkyl(aralkyl)-3-methyl(ethyl)imidazolium halides: Precursors for room-temperature ionic liquids. *J. Heterocyclic Chem.*, **38**, 265-268 (2001).

[DOI: 10.1002/jhet.5570380139](https://doi.org/10.1002/jhet.5570380139)

[23] Ennis E., Handy T. S. Facile route to C₂-substituted imidazolium ionic liquids. *Molecules*, **14**, 2235-2245 (2009).

[DOI: 10.3390/molecules14062235](https://doi.org/10.3390/molecules14062235)

[24] Denk M. K., Ye X. Alkylation of ethylenethiourea with alcohols: a convenient synthesis of S-alkyl-isothioureas without toxic alkylating agents. *Tetrahedron Lett.*, **46**, 7597-7599 (2005).

[DOI: 10.1016/j.tetlet.2005.08.150](https://doi.org/10.1016/j.tetlet.2005.08.150)

[25] Van Krevelen D. W. Properties of polymers: their correlation with chemical structure: their numerical estimation and prediction from additive group contributions. Elsevier, Amsterdam (2009).

- [26] Vogel H. Das temperaturabhängigkeit gesetz der viskosität von flüssigkeiten. Phys. Z., **22**, 645-646 (1921).
- [27] Fulcher G. S. Analysis of recent measurements of the viscosity of glasses. J. Am. Ceram. Soc., **8**, 789-794 (1925).
[DOI:10.1111/j.1151-2916.1925.tb18582.x](https://doi.org/10.1111/j.1151-2916.1925.tb18582.x)
- [28] Tammann G., Hesse W. Die abhängigkeit der viskosität von der temperatur bei unterkühlten flüssigkeiten. Z. Anorg. Allg. Chem., **156**, 245-257 (1926).
[DOI:10.1002/zaac.19261560121](https://doi.org/10.1002/zaac.19261560121)
- [29] Williams M. L., Landel R. F., Ferry J. D. The temperature dependence of relaxation mechanisms in amorphous polymers and other glass-forming liquids. J. Am. Chem. Soc., **77**, 3701-3707 (1955).
[DOI: 10.1021/ja01619a008](https://doi.org/10.1021/ja01619a008)
- [30] Li G., Lee-Sullivan P., Thring R. W. Determination of activation energy for glass transition of an epoxy adhesive using dynamic mechanical analysis. J. Therm. Anal. Calorim., **60**, 377-390 (2000).
[DOI: 10.1023/A:1010120921582](https://doi.org/10.1023/A:1010120921582)
- [31] Fainleib A., Grigoryeva O., Starostenko O., Vashchuk A., Rogalsky S., Grande D. Acceleration effect of ionic liquids on polycyclotrimerization of dicyanate esters. eXPRESS Polym. Lett., **10**, 722-729 (2016).
[DOI: 10.3144/expresspolymlett.2016.66](https://doi.org/10.3144/expresspolymlett.2016.66)
- [32] Bershtein V. A., David L., Egorov V. M., Fainleib A. M., Grigorieva O., Bey I., Yakushev P. N. Structural/compositional nanoheterogeneity and glass transition plurality in amorphous polycyanurate-poly(tetramethylene glycol) hybrid networks. J. Polym. Sci.: Part B: Polym. Phys., **43**, 3261-3272 (2005).
[DOI: 10.1002/polb.20614](https://doi.org/10.1002/polb.20614)
- [33] Fainleib A., Grigoryeva O., Hourston D. Synthesis of inhomogeneous modified polycyanurates by reactive blending of bisphenol A dicyanate ester and polyoxypropylene glycol. Macromol. Symp., **164**, 429-442 (2001).
[DOI: 10.1002/1521-3900\(200102\)164:1<429::AID-MASY429>3.0.CO;2-I](https://doi.org/10.1002/1521-3900(200102)164:1<429::AID-MASY429>3.0.CO;2-I)
- [34] Fainleib A., Hourston D., Grigoryeva O., Shantalii T., Sergeeva L. Structure development in aromatic polycyanurate networks modified with hydroxyl-terminated polyethers. Polymer, **42**, 8361-8372 (2001).
[DOI: 10.1016/S0032-3861\(01\)00333-0](https://doi.org/10.1016/S0032-3861(01)00333-0)

[35] Fainleib A. M., Grigoryeva O. P., Hourston D. J. Structure-Properties Relationships for Bisphenol A Polycyanurate Network Modified with Polyoxytetramethylene Glycol. *Int. J. Polym. Mat.*, **51**, 57-75 (2001).

[DOI: 10.1080/00914030213025](https://doi.org/10.1080/00914030213025)

[36] Grigat E., Putter R. Chemie der Cyansaureester. IV. Umsetzung von Cyansaureestern mit imino- bzw. iminogruppenhaltigen substanzen. *Chem. Ber.*, **11**, 3027-3035 (1964).

[DOI: 10.1002/cber.19640971110](https://doi.org/10.1002/cber.19640971110)

[37] Bauer J., Bauer M. Curing of cyanates with primary amines. *Macromol. Chem. Phys.*, **202**, 2213-2220 (2001).

[DOI: 10.1002/1521-3935\(20010701\)202:11<2213::AID-MACP2213>3.0.CO;2-B](https://doi.org/10.1002/1521-3935(20010701)202:11<2213::AID-MACP2213>3.0.CO;2-B)

[38] Nyquist R. A., Putzig C. L., Torrey D. Clark. Infrared study of 1,3-dimethyl-2-imidazolidinone in various solvents. *Vibrational Spectroscopy*, **12**, 81-91 (1996).

[DOI: 10.1016/0924-2031\(96\)00004-5](https://doi.org/10.1016/0924-2031(96)00004-5)

[39] Piasek Z., Urbanski T. The infra-red absorption spectrum and structure of urea. *Bulletin de l'Académie Polonaise des Sciences*, **10**, 113-120 (1962).

[40] Arshad M. N., Bibi A., Mahmood T., Asiri A. M., Ayub K. Synthesis, crystal structures and spectroscopic properties of triazine-based hydrazone derivatives; A comparative experimental-theoretical study. *Molecules*, **20**, 5851-5874 (2015).

[DOI: 10.3390/molecules20045851](https://doi.org/10.3390/molecules20045851)

[41] Guo R., Sanders D. F., Smith Z. P., Freeman B. D., Paul D. R., McGrath J. E. Synthesis and characterization of thermally rearranged (TR) polymers: effect of glass transition temperature of aromatic poly(hydroxyimide) precursors on TR process and gas permeation properties. *J. Mater. Chem. A*, **1**, 6063-6072 (2013).

[DOI: 10.1039/c3ta10261k](https://doi.org/10.1039/c3ta10261k)

[42] Kimura H., Ohtsuka K., Matsumoto A. Curing reaction of bisphenol-A based benzoxazine with cyanate ester resin and the properties of the cured thermosetting resin. *eXPRESS Polym. Lett.*, **5**, 1113-1122 (2011).

[DOI: 10.3144/expresspolymlett.2011.108](https://doi.org/10.3144/expresspolymlett.2011.108)

[43] Korshak V. V., Gribkova P. N., Dmitrenko A. V., Puchin A. G., Pankratov V. A., Vinogradova S. V. Thermal and thermal-oxidative degradation of polycyanates. *Polym. Sci. U.S.S.R.*, **16**, 15-23 (1974).

[DOI: 10.1016/0032-3950\(74\)90111-7](https://doi.org/10.1016/0032-3950(74)90111-7)

[44] Ramirez M. L., Walters R., Savitski E. P., Lyon R. E. Thermal decomposition of cyanate ester resins. *Polym. Degrad. Stab.*, **78**, 73-82 (2002).

[DOI: 10.1016/S0141-3910\(02\)00121-0](https://doi.org/10.1016/S0141-3910(02)00121-0)

[45] Ward I. M., Hadley D. W. An introduction to the mechanical properties of solid polymers. Wiley, New York (1993).

[46] Lafia O. A., Imrana M. M. A., Abdullah M. K. Glass transition activation energy, glass-forming ability and thermal stability of $\text{Se}_{90}\text{In}_{10-x}\text{Sn}_x$ ($x = 2, 4, 6$ and 8) chalcogenide glasses. *Physica B: Condensed Matter*, **395**, 69-75 (2007).

[DOI: 10.1016/j.physb.2007.02.026](https://doi.org/10.1016/j.physb.2007.02.026)

[47] Bershtein V., Fainleib A., Yakushev P. Polycyanurate-based hybrid networks and nanocomposites: structure-glass transition dynamics-dynamic heterogeneity-properties relationships. In “*Thermostable polycyanurates. Synthesis, modification, structure and properties*”. Nova Science Publishers, New York, 2010. Chapter 7, p. 195-246.

Table 1. Chemical structure and basic physico-chemical characteristics of components under investigation

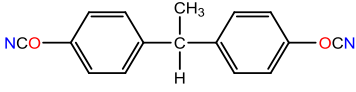
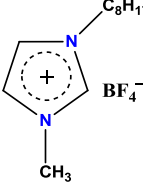
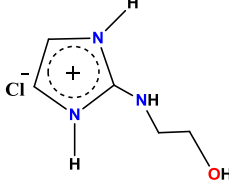
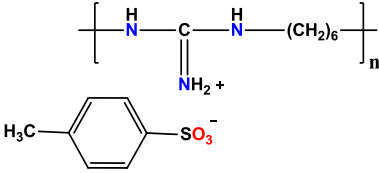
Component	Structure	Characteristics
<i>1,1-bis(4-cyanatophenyl)ethane</i> DCBE		$M = 264 \text{ g/mol}$ $T_m \approx 29^\circ\text{C}$ $T_d \approx 434^\circ\text{C}$ $\delta = 24.5 \text{ (J/cm}^3)^{1/2}$
<i>1-octyl-3-methylimidazolium tetrafluoroborate</i> [OMIm][BF ₄]		$M = 282 \text{ g/mol}$ $T_m \approx -88^\circ\text{C}$ $T_d \approx 401^\circ\text{C}$ $\delta = 18.8 \text{ (J/cm}^3)^{1/2}$
<i>2-(hydroxyethylamino)imidazolinium chloride</i> [HEAIm][Cl]		$M = 164 \text{ g/mol}$ $T_m \approx 97\text{-}98^\circ\text{C}$ $T_d \approx 244^\circ\text{C}$ $\delta = 28.9 \text{ (J/cm}^3)^{1/2}$
<i>Polyhexamethylene guanidine toluene sulfonate</i> [PHMG][TS]		$M_n = 12,520 \text{ g/mol (n} \sim 40\text{-}50)$ $T_m \approx 110\text{-}115^\circ\text{C}$ $T_d \approx 371^\circ\text{C}$ $\delta = 25.6 \text{ (J/cm}^3)^{1/2}$

Table 2. Kinetic parameters of DCBE polymerization in the absence and the presence of 1.0 wt.% IL

Network	t_i^a (min)	$W_{\max} \times 10^3^b$ (min ⁻¹)	t_{\max}^c (min)	α_c^d (%)
Neat CER	60	8.4	89	89
CER / [OMIm][BF ₄]	20	10.2	52	91
CER / [HEAIm][Cl]	34	9.7	68	82
CER / [PHMG][TS]	40	9.2	83	78

^a induction period

^b maximal rate of reaction ($W = d\alpha/dt$)

^c time to maximal rate of reaction

^d maximal conversion of $-O-C\equiv N$ groups

Table 3. Thermal stability of CER-based networks and pure ILs as investigated by TGA

Sample	$T_{d\text{ onset}}^a$ (°C)	$T_{d\text{ max}}^b$ (°C)	Δm^c (%)	Char residue at 680°C (%)
Neat CER	427	441	33.7	47.5
CER / [OMIm][BF ₄]	425	443	33.1	46.7
CER / [HEAIm][Cl]	424	443	35.1	45.7
CER / [PHMG][TS]	420	438	34.3	45.4
[OMIm][BF ₄]	396	439	91.3	0.0
[HEAIm][Cl]	240	295	94.2	1.3
[PHMG][TS]	372	403	78.1	13.0

^a $T_{d\text{ onset}}$: onset temperature for intensive degradation stage considered

^b $T_{d\text{ max}}$: temperature of maximum degradation rate for intensive stage considered

^c Δm : mass loss for intensive degradation stage considered

Table 4. Viscoelastic properties of CER-based networks as investigated by DMTA

Network	T_{α}^a (°C)	$\tan \delta_{\max}$	ΔT^b (°C)	ΔE_a^c (kJ/mol)	E' (GPa)			$T_{\text{pc}(\text{onset})}^d$ (°C)
					20°C	200°C	250°C	
CER	263	0.38	33	292	2.2	1.6	0.60	288
CER / [OMIm][BF ₄]	262	0.52	40	286	2.1	1.4	0.56	277
CER / [HEAIm][Cl]	248	0.67	40	255	2.3	1.5	0.10	268
CER / [PHMG][TS]	242	0.68	42	196	1.6	0.8	0.02	260

^a T_{α} : α relaxation temperature^b ΔT : temperature width at $\frac{1}{2} \tan \delta_{\max}$ height^c ΔE_a : apparent activation energy of α relaxation^d $T_{\text{pc}(\text{onset})}$: onset of temperature of CER post-curing as determined from $E' = f(T)$

Figure Captions

Figure 1. Reaction scheme of DCBE polycyclotrimerization

Figure 2. Typical FTIR spectra in $2320\text{--}1290\text{ cm}^{-1}$ region during curing procedure for: (a) neat CER, (b) CER/[OMIm][BF₄], (c) CER/[HEAIm][Cl], and (d) CER/[PHMG][TS]. The spectra were shifted vertically for the sake of clarity

Figure 3. Kinetic curves at $T = 150\text{ }^{\circ}\text{C}$: time dependence of (a) conversion (α_c) of --OCN groups from DCBE and (b) reaction rate (da/dt). Neat CER (1), CER/[OMIm][BF₄] (2), CER/[HEAIm][Cl] (3), and DCBE/[PHMG][TS] (4)

Figure 4. FTIR spectra in $1780\text{--}1350\text{ cm}^{-1}$ region for: (1) neat CER, (2) [OMIm][BF₄], (3) CER/[OMIm][BF₄] 50/50 wt.%, (4) [HEAIm][Cl], (5) DCBE/[HEAIm][Cl] 50/50 wt.% before curing, (6) CER/[HEAIm][Cl] 50/50 wt.% after curing, (7) [PHMG][TS], (8) DCBE/[PHMG][TS] 50/50 wt.% before curing, (9) CER/[PHMG][TS] 50/50 wt.% after curing. The spectra were shifted vertically for the sake of clarity

Figure 5. Proposed mechanism for [OMIm][BF₄]-catalyzed DCBE polycyclotrimerization

Figure 6. Proposed mechanism for [HEAIm][Cl]-catalyzed DCBE polycyclotrimerization

Figure 7. Proposed mechanism for [PHMG][TS]-catalyzed DCBE polycyclotrimerization

Figure 8. Chemical reaction between cyanate groups of DCBE and traces of water or phenol impurity accompanying the DCBE monomer

Figure 9. TGA curves for CER-based networks (a) and pure ILs (b): neat CER (-), CER/[OMIm][BF₄] (-●-), CER/[HEAIm][Cl] (-■-), CER/[PHMG][TS] (-▲-), [OMIm][BF₄] (-○-), [HEAIm][Cl] (-□-), and [PHMG][TS] (-△-)

Figure 10. Plot of E' (a) and $\tan\delta$ (b) as a function of temperature at 1 Hz for: CER (-), CER/[OMIm][BF₄] (-●-), CER/[HEAIm][Cl] (-■-), and CER/[PHMG][TS] (-▲-)

Figure 11. Plot of $\log f$ vs. $1000/T$ for: CER (-), CER/[OMIm][BF₄] (-●-), CER/[HEAIm][Cl] (-■-), and CER/[PHMG][TS] (-▲-)

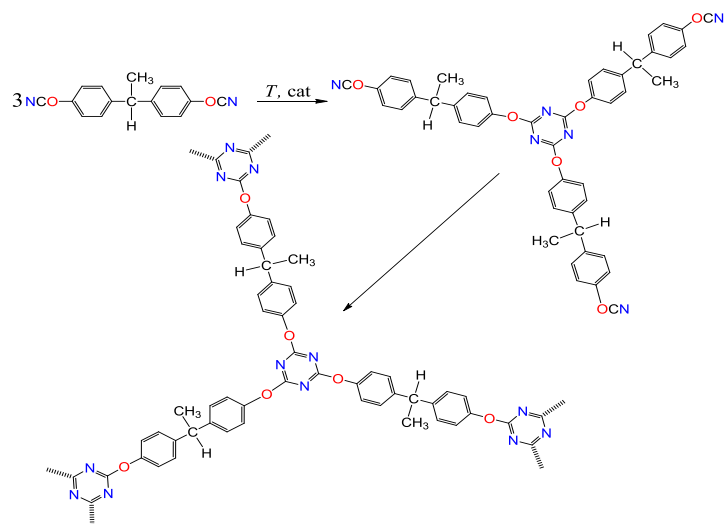


Figure 1.

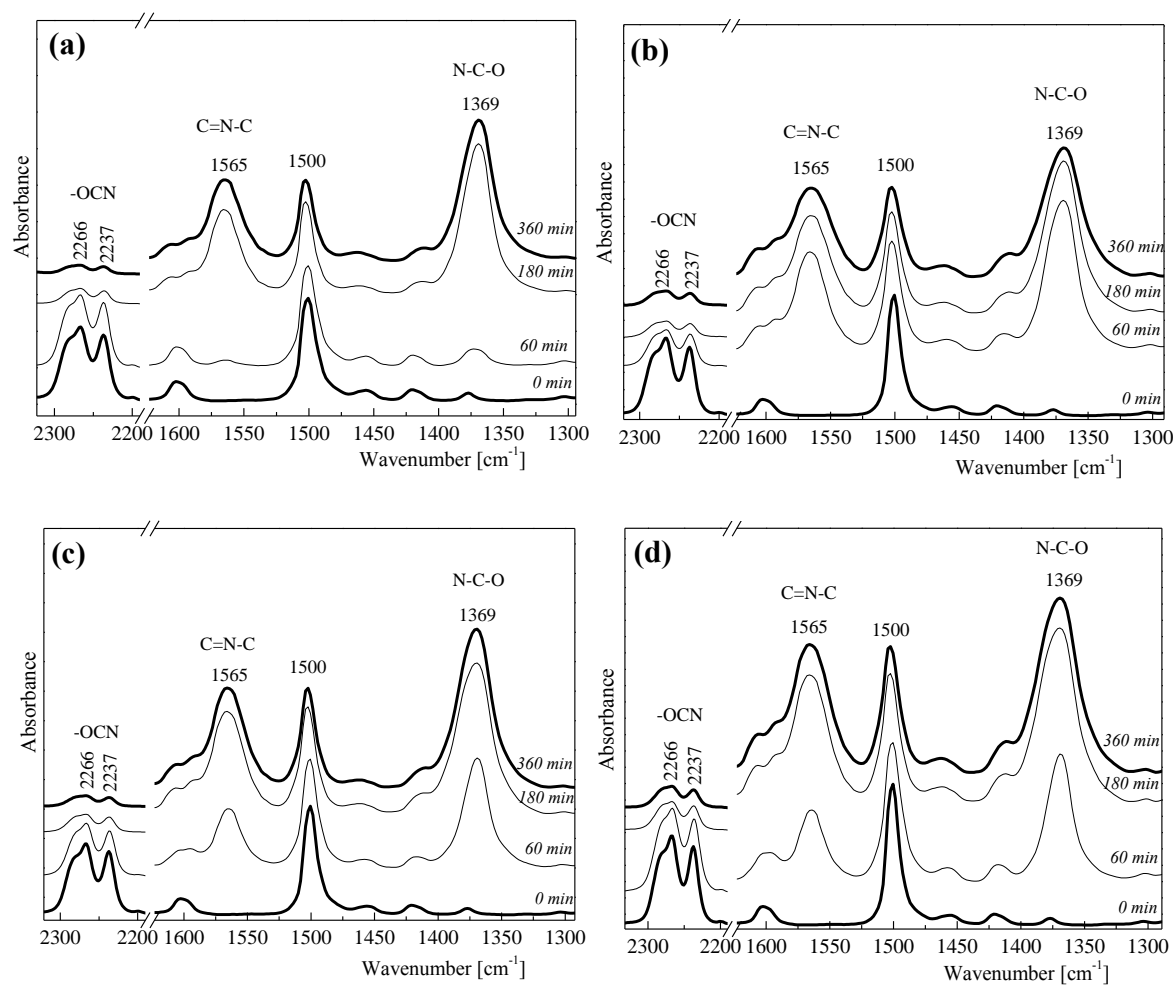


Figure 2.

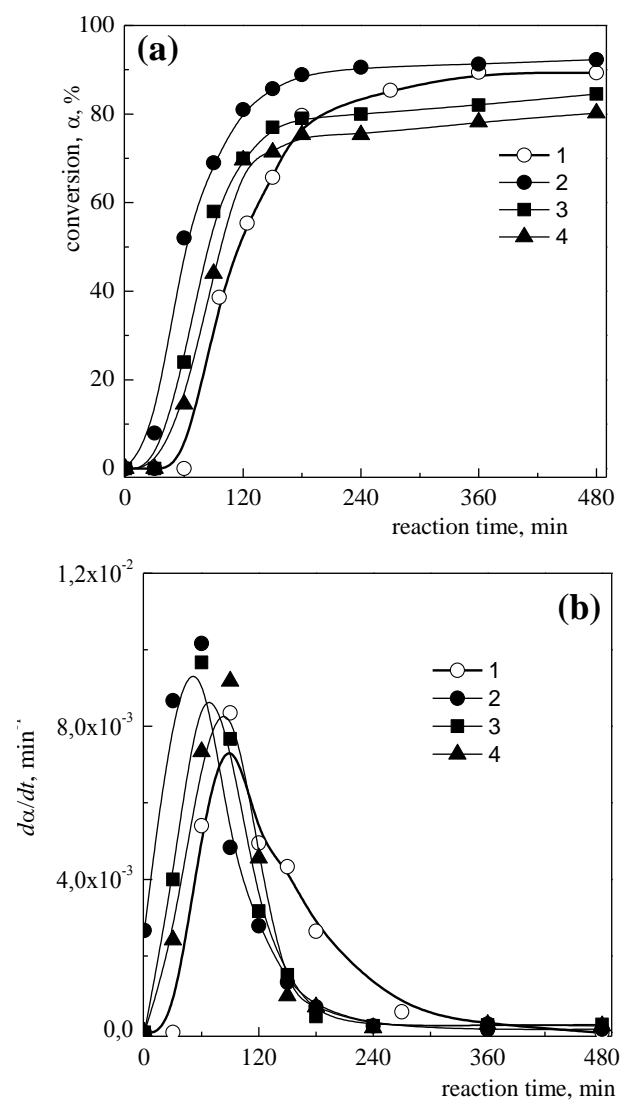


Figure 3.

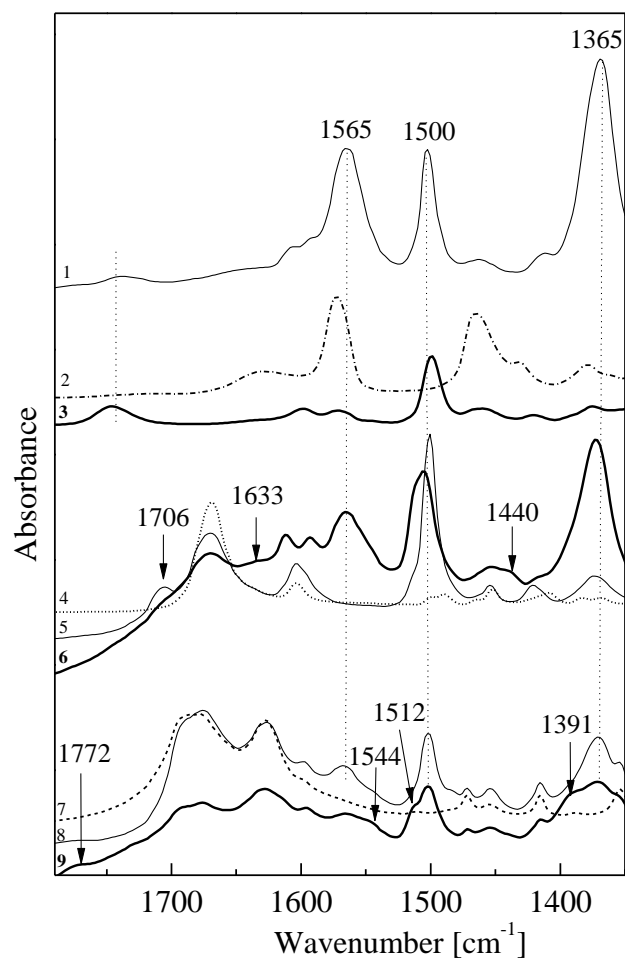


Figure 4.

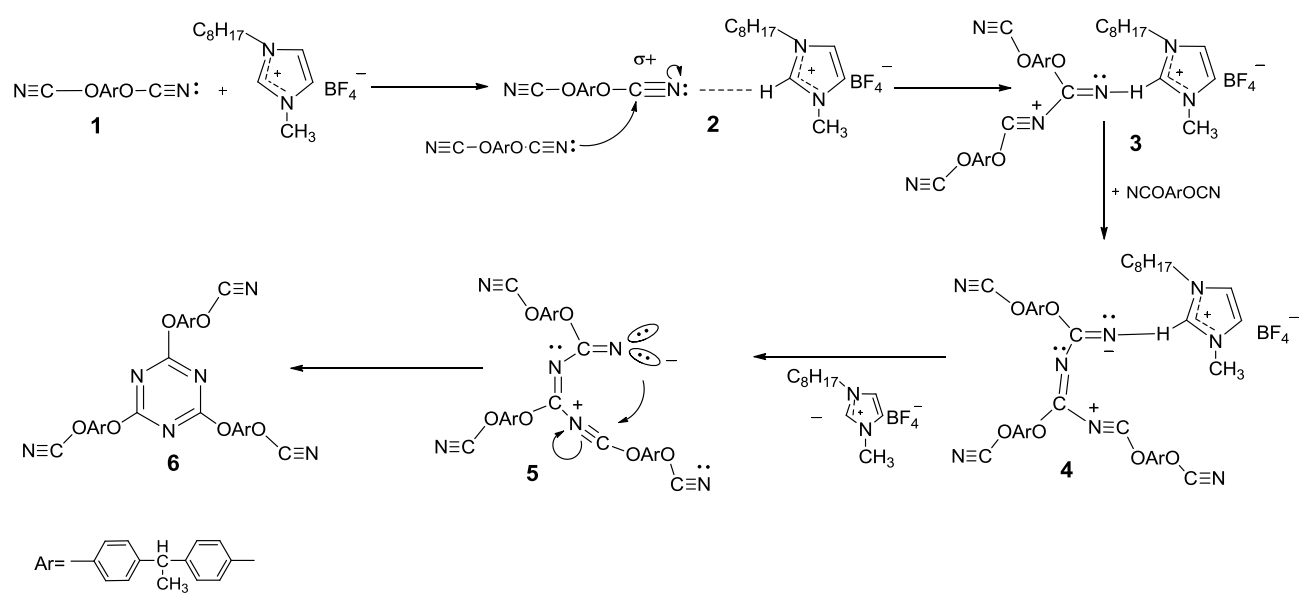


Figure 5.

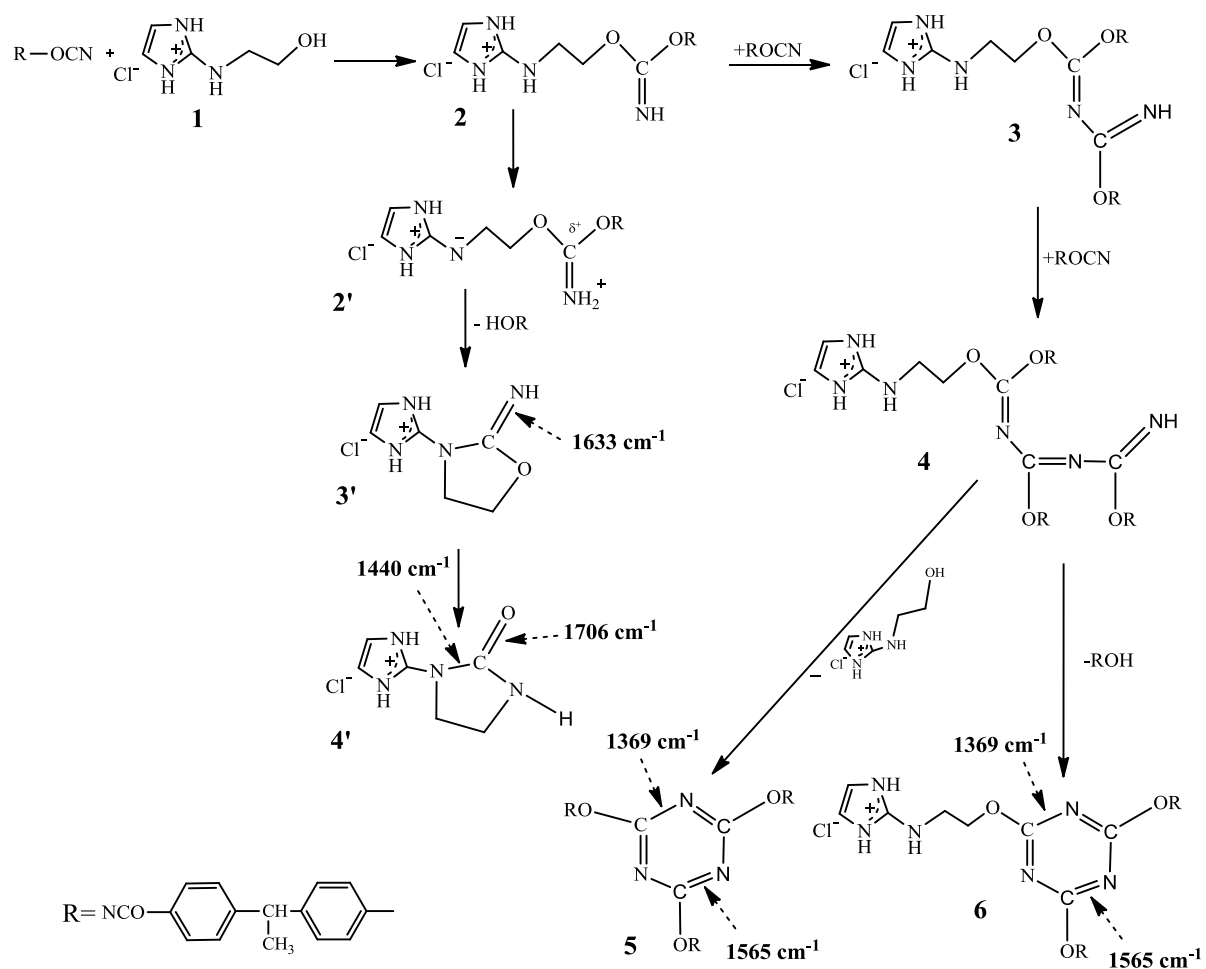


Figure 6.

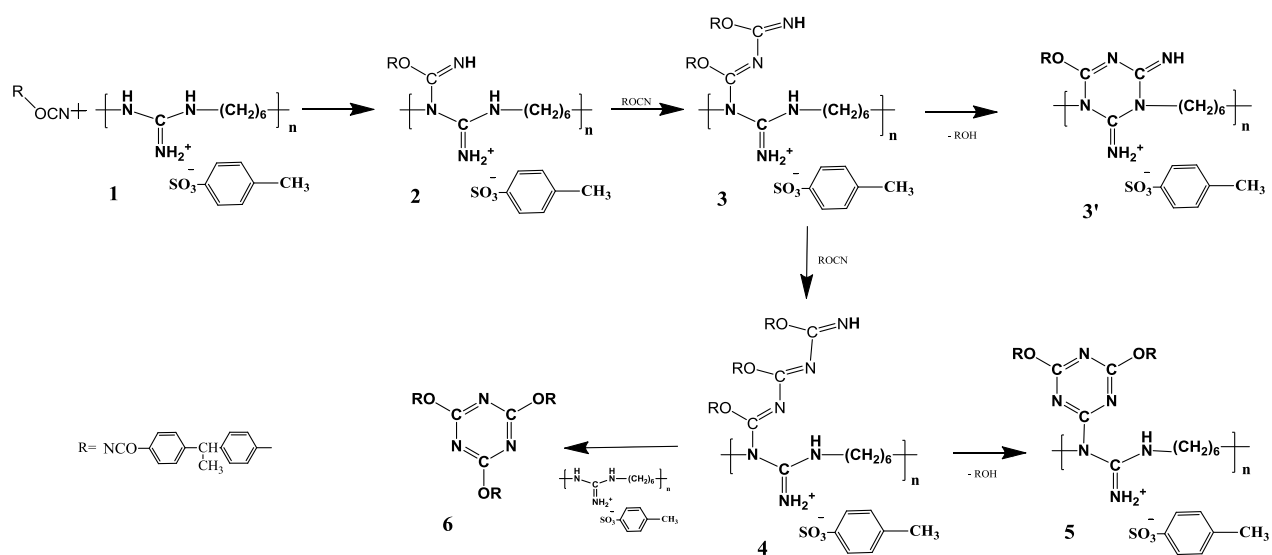


Figure 7.

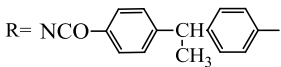


Figure 8.

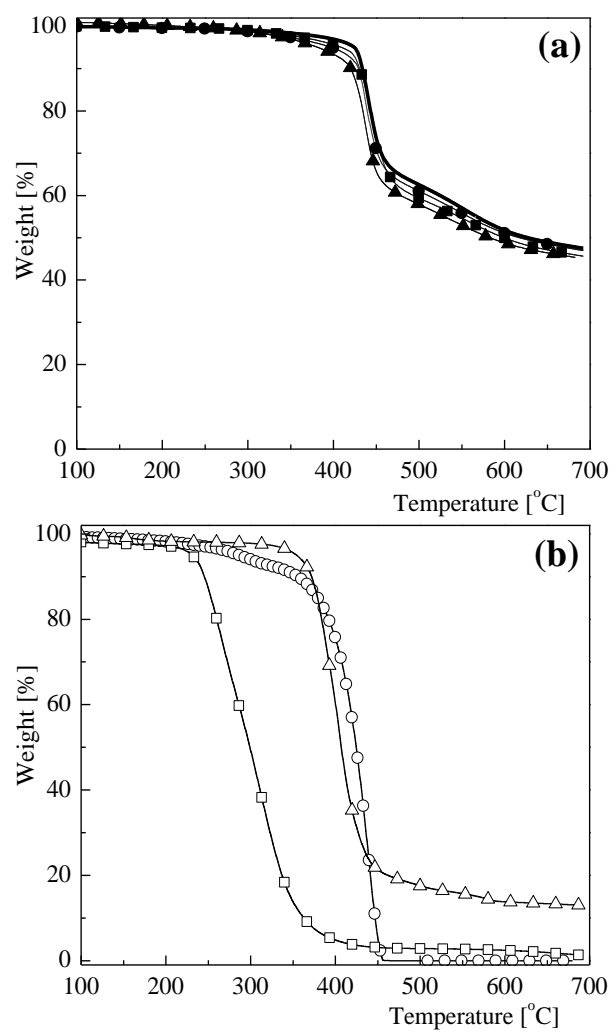


Figure 9.

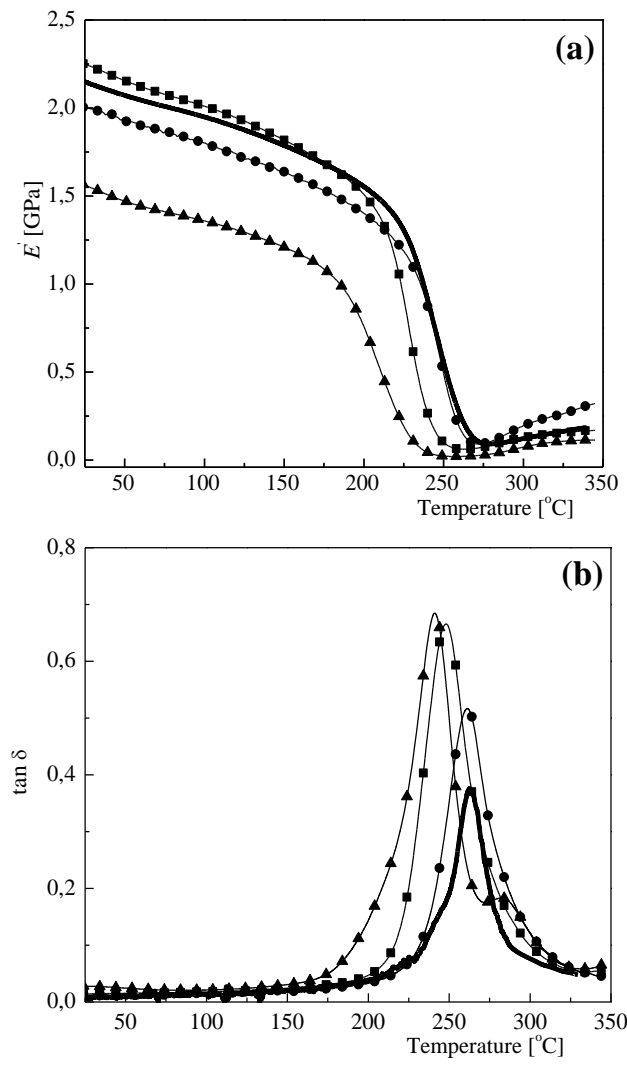


Figure 10.

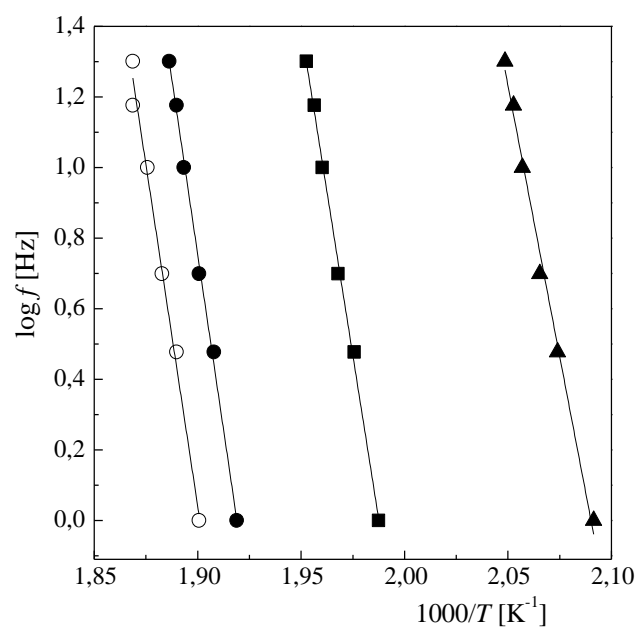


Figure 11.